

DESY 95-205
FNT/T-95/28
LNF-95/059(P)
MPI/PhT/95-113
 December 1995

Large- p_{\perp} Heavy-Quark Production in Two-Photon Collisions

M. CACCIARI^{a†}, M. GRECO^b, B.A. KNIEHL^c, M. KRÄMER^a, G. KRAMER^d, M. SPIRA^d

^aDeutsches Elektronen-Synchrotron DESY, 22603 Hamburg, Germany

^bDipartimento di Fisica, Università di Roma III, and
INFN, Laboratori Nazionali di Frascati, Italy

^cMax-Planck-Institut für Physik, Föhringer Ring 6, 80805 Munich, Germany

^dII. Institut für Theoretische Physik[‡], Universität Hamburg, 22761 Hamburg, Germany

Abstract

The next-to-leading-order (NLO) cross section for the production of heavy quarks at large transverse momenta (p_{\perp}) in $\gamma\gamma$ collisions is calculated with perturbative fragmentation functions (PFF's). This approach allows for a resummation of terms $\propto \alpha_s \ln(p_{\perp}^2/m^2)$ which arise in NLO from collinear emission of gluons by heavy quarks at large p_{\perp} or from almost collinear branching of photons or gluons into heavy-quark pairs. We present single-inclusive distributions in p_{\perp} and rapidity including direct and resolved photons for $\gamma\gamma$ production of heavy quarks at e^+e^- colliders and at high-energy $\gamma\gamma$ colliders. The results are compared with the fixed-order calculation for m finite including QCD radiative corrections. The two approaches differ in the definitions and relative contributions of the direct and resolved terms, but essentially agree in their sum. The resummation of the $\alpha_s \ln(p_{\perp}^2/m^2)$ terms in the PFF approach leads to a softer p_{\perp} distribution and to a reduced sensitivity to the choice of the renormalization and factorization scales.

[†] Della Riccia and Università di Pavia fellow. Work also supported by INFN, Sezione di Pavia.

[‡] Supported by Bundesministerium für Forschung und Technologie, Bonn, Germany, Contract 05 6 HH 93P (5) and EEC Program *Human Capital and Mobility* through Network *Physics at High Energy Colliders* under Contract CHRX-CT93-0357 (DG12 COMA).

1. Introduction

A large number of equivalent photons is generated at high-energy e^+e^- colliders, giving rise to the production of heavy-quark pairs in two-photon collisions. This process has been studied for charmed particles by several experiments at PETRA, PEP, TRISTAN, and LEP [1]. At LEP2, a total of $\sim 350\,000\ c\bar{c}$ and $\sim 1500\ b\bar{b}$ pairs will be produced in $\gamma\gamma$ collisions for an integrated luminosity of $\int \mathcal{L} = 500\ \text{pb}^{-1}$ [2]. The yield of heavy quarks at high-energy e^+e^- linear colliders is even higher, depending in detail on the spectrum of the beamstrahlung photons, which strongly varies with the machine design and operation. If the novel method of Compton back-scattering of laser light can be made work [3], it will be possible to generate high-luminosity beams of real photons carrying $\sim 80\%$ of the electron/positron energy. The high-statistics data from the future experimental facilities will allow for a detailed comparison of the next-to-leading order (NLO) predictions with experimental results not only for total production rates, but also for various differential distributions. These analyses will provide us with information on the dynamics of heavy-flavour production in a kinematical range very different from that available in $\gamma\gamma$ collisions at present colliders.

Three mechanisms contribute to the production of heavy quarks in $\gamma\gamma$ collisions: (i) In the case of direct (DD) production, the two photons couple directly to the heavy quarks. No spectator particles travel along the γ axes. (ii) If one of the photons first splits into a flux of light quarks and gluons [4], one of the gluons may fuse with the second photon to form the $Q\bar{Q}$ pair. The remaining light quarks and gluons build up a spectator jet in the split- γ direction (single-resolved (DR) γ contribution). The total $\gamma\gamma$ cross section of this mechanism depends on the parton density functions (PDF's) of the photon [5–7]. (iii) If both photons split into light quarks and gluons, the $Q\bar{Q}$ pair is accompanied by two spectator jets (double-resolved (RR) γ contribution). Since the photon PDF's scale as $\alpha\alpha_s^{-1}$, the DR and RR processes are of the same order as the DD process.

Many features of the above-mentioned production mechanisms are calculable in perturbative QCD. The mass of the heavy quark, $m \gg \Lambda_{\text{QCD}}$, acts as a cutoff and sets the scale for the perturbative calculations. The production cross section factorizes into a partonic hard-scattering cross section multiplied by light-quark and gluon PDF's [8]. Inherent in this factorization scheme is the notion that the only quarks in the photon are the light ones. There are no contributing subprocesses initiated by an intrinsic heavy flavour coming directly from the photon PDF's. In leading order (LO), direct production is described by the partonic reaction $\gamma + \gamma \rightarrow c + \bar{c}$ while the resolved contributions involve the channels $g + \gamma \rightarrow c + \bar{c}$ (DR) and $q + \bar{q} \rightarrow c + \bar{c}$, $g + g \rightarrow c + \bar{c}$ (RR), where q are light (massless) flavours [9]. The NLO corrections to these processes have been calculated and found to be substantial [2,10,11,12]. A comparison between the NLO results and experimental data on the total cross section of charm-quark production in two-photon collisions has shown satisfactory agreement [13].

One might expect that the massive approach is reasonable only in those kinematical regions where the mass m and any other characteristic energy scale like p_\perp are approximately of the same magnitude and significantly larger than Λ_{QCD} . In NLO, terms $\propto \alpha_s \ln(p_\perp^2/m^2)$ arise from collinear emission of gluons by heavy quarks at large transverse momenta (p_\perp) or from almost collinear branching of gluons or photons into heavy-quark pairs. These terms are not expected to affect the total production rates, but they might spoil the convergence of the perturbation series and cause

large scale dependences of the NLO result at $p_{\perp} \gg m$.¹ In the massive approach, the prediction of differential cross sections is thus limited to a rather small range of $p_{\perp} \sim m$. An alternative way of making predictions at large p_{\perp} is to treat the heavy quarks as massless partons. The mass singularities of the form $\ln(p_{\perp}^2/m^2)$ are then absorbed into the PDF's and fragmentation functions (FF's) in the same way as for the light u , d , and s quarks. The crucial difference to the production of light hadrons is the fact that the initial-state conditions for the heavy-quark FF's can be calculated within perturbative QCD and do not have to be taken from experiment [15]. Such perturbative fragmentation functions (PFF's) have been used in Ref. [16] to study the production of large- p_{\perp} bottom quarks in $p\bar{p}$ collisions. Meanwhile, similar analyses have been carried out for charm-quark production in photon-proton collisions at HERA [17,18]. In the massless scheme, the heavy quark is, of course, considered to be one of the massless active flavours in the photon PDF's. We expect the massless PFF approach to be better suited for the calculation of the differential p_{\perp} distributions at NLO in the region $p_{\perp} \gg m$. The small- p_{\perp} region is, however, not calculable without retaining the full m dependence. The massless cross section diverges in the limit $p_{\perp} \rightarrow 0$, and total production rates can not be predicted.

At this point, it is worth mentioning that the massive and the massless approaches are expected to give different descriptions of the DD, DR, and RR contributions. In the massive approach, the direct and resolved contributions are separately well defined through NLO. In fact, there is no need to perform any factorization for the incoming photons. This means that an experiment analyzing data without hadronic activity in the directions of the incoming photons would directly probe the NLO calculation of DD heavy-quark production. This is, however, not true in the massless approach. If the charm is treated as a massless parton, the photon splitting to $c\bar{c}$ must also undergo a subtraction procedure. The DD piece then becomes factorization-scheme dependent and loses its direct physical interpretation. Consequently, the same is true for the DR and RR parts. As a matter of principle, the three contributions cannot be experimentally separated any more with NLO accuracy. Only their sum corresponds to a physical observable. On the other hand, if one were to extend the massive approach up to large p_{\perp} , the DD prediction would, of course, still be unambiguously defined, but it would be affected by large logarithmic terms, which would render it unreliable. Only at moderate $p_{\perp} \sim m$ and through NLO, it is therefore possible to probe the theoretical predictions for direct and resolved contributions separately by an experimental analysis.

In the near future, we expect experimental data in the intermediate p_{\perp} range, where $p_{\perp} > m$ rather than $p_{\perp} \gg m$. Then, the problem how to proceed in this p_{\perp} region arises. In order to investigate the region where $p_{\perp} > m$, we calculate the differential cross section $d^2\sigma/dy dp_{\perp}^2$ as a function of p_{\perp} with fixed rapidity y . We compare the results in the two approaches: (i) the massive-charm approach with $m = 1.5$ GeV, in which we compute the cross section for open charm production, and (ii) the massless approach, where we evaluate the same differential cross section for inclusive charm production using PFF's. In both calculations, we include the DD, DR, and RR processes up to NLO. The massive calculation is based on the work presented in [2], in which the NLO theory for DD and DR production was elaborated. The calculation of the massive RR cross section relies on the work of [10,11]. The massless calculation proceeds along the lines of [16–19] on the basis of the DR and RR hard-scattering cross sections obtained in [20,21]. The NLO corrections

¹Similar potentially large terms $\propto \alpha_s \ln(Q^2/m^2)$, Q being the photon virtuality, do appear in NLO calculations of heavy quark electroproduction cross sections. The resummation of these logarithms is being considered in a series of papers [14].

to the DD cross section were derived in [22] and recently confirmed in [23]. In the massless approach, we adopt the PFF's calculated in [15]. With this choice of PFF's, the LO results in the massive scheme approach the LO massless results in the limit $m \rightarrow 0$, if we restrict ourselves to the same parton subprocesses. In LO, the PFF's are equal to $\delta(1-x)$ (see Eq. (1)) showing that, in LO, we have full correspondence between the massless and massive approaches. However, they must differ in NLO, where the limit $m \rightarrow 0$ is not possible due to the unabsorbed mass-singular $\ln(p_\perp^2/m^2)$ terms in the massive approach. In the massless approach, these terms are contained in the higher-order terms of the photon PDF's and the PFF's. This situation is very similar to our previous study for photon-proton collisions at HERA [17,18]. Indeed the direct and resolved contributions in γp scattering correspond to the DR and RR contributions in $\gamma\gamma$ collisions with the proton PDF's replaced by the photon PDF's. In addition, we now have the DD contribution.

The outline of our work is as follows. In Section 2, we shortly describe the basic formalism for the massless PFF approach. Section 3 contains the numerical results. Our conclusions are summarized in Section 4.

2. The perturbative fragmentation function approach

In this section, we describe in some detail the PFF approach to heavy-quark production at large p_\perp . This technique was proposed in [11] and first applied in the context of hadron collisions for describing large- p_\perp bottom production [16]. The basic assumption is that when a large scale is governing the production process (in our case, this is p_\perp , with $p_\perp \gg m$) the heavy quark itself is produced as if it was massless. Technically speaking, non-singular mass terms are suppressed in the cross section by powers of m/p_\perp . The important mass terms appear whenever the virtuality of the heavy quark is small. This happens in the initial state when the heavy parton is emitted from the colliding hadron, and in the final state when the partons materialize into a massive quark.

This qualitative picture of heavy-quark production in the large- p_\perp limit can be substantiated at NLO in the following way: (i) The hard-scattering cross sections are calculated in the massless approximation, and the collinear singularities are subtracted according to some factorization scheme, *e.g.*, the $\overline{\text{MS}}$ scheme. Since the heavy parton is taken to be massless, also the singularities arising from its splittings are subtracted. (ii) As for the initial state, the heavy parton is accommodated in the PDF's like a light flavour. The massiveness of the quark is usually taken into account by including it in the evolution only above a scale set by its mass. (iii) As for the final state, the PFF's characterize the hadronization of the massless partons into the heavy-quark state. Exploiting the fact that the produced quark has mass $m \gg \Lambda_{\text{QCD}}$, universal starting conditions for these FF's can be calculated within perturbative QCD (therefore they are denoted PFF's) at a scale μ_0 of order m . In [15], these starting conditions were calculated at NLO in the $\overline{\text{MS}}$ scheme. They read

$$\begin{aligned}
D_Q^Q(x, \mu_0) &= \delta(1-x) + \frac{\alpha_s(\mu_0)}{2\pi} C_F \left\{ \frac{1+x^2}{1-x} \left[\log \frac{\mu_0^2}{m^2} - 2 \log(1-x) - 1 \right] \right\}_+, \\
D_g^Q(x, \mu_0) &= \frac{\alpha_s(\mu_0)}{2\pi} T_f [x^2 + (1-x)^2] \log \frac{\mu_0^2}{m^2}, \\
D_{q,\bar{q},\bar{Q}}^Q(x, \mu_0) &= 0,
\end{aligned} \tag{1}$$

where D_a^Q refers to the fragmentation of parton a into the heavy quark Q , $C_F = 4/3$, and $T_f = 1/2$.

(*iv*) Finally, the PDF's and PFF's are evolved in NLO up to the chosen factorization scale (which is usually of the order of p_\perp) via the Altarelli-Parisi equations and convoluted with the hard-scattering cross sections. Notice that, in this approach, the heavy-quark mass enters the calculation only via the starting conditions of the PDF's and PFF's.

In this framework, the large logarithmic terms are resummed in the following way. The would-be mass singularities $\propto \ln(p_\perp^2/m^2)$ are split into two parts. One part $\propto \ln(p_\perp^2/\mu^2)$, where μ is the factorization scale, appears in the hard-scattering cross sections, which have no dependence on m . This part may be eliminated by choosing $\mu \sim p_\perp$. The other part $\propto \ln(\mu^2/m^2)$ is absorbed into the PFF's. The large $\ln(\mu^2/\mu_0^2)$, with $\mu_0 \sim m$ and $\mu \sim p_\perp$, is implemented via the evolution equations, and therefore these large logarithms are resummed. The residual terms $\propto \ln(m^2/\mu_0^2)$ connected with the starting condition in Eq. (1) are treated at fixed order in perturbation theory.

3. Results

In the following, we collect our results for the cross section $d^2\sigma/dy dp_\perp^2$ for three cases of particular interest: (*i*) LEP2 with $\sqrt{s} = 175$ GeV, (*ii*) Next Linear Collider (NLC) with $\sqrt{s} = 500$ GeV assuming the TESLA design, and (*iii*) NLC with $\sqrt{s} = 500$ GeV operated in the $\gamma\gamma$ mode implemented by backscattering of laser light on the e^+ and e^- beams.

We start with our analysis relevant for LEP2. The quasi-real-photon spectrum is described in the Weizsäcker-Williams approximation (WWA) by the formula [24]

$$f_\gamma(x) = \frac{\alpha}{2\pi} \left\{ \frac{1 + (1-x)^2}{x} \ln \frac{E^2\theta_c^2(1-x)^2 + m_e^2x^2}{m_e^2x^2} + 2(1-x) \left[\frac{m_e^2x}{E^2\theta_c^2(1-x)^2 + m_e^2x^2} - \frac{1}{x} \right] \right\}, \quad (2)$$

where $x = E_\gamma/E_e$ is varied over the full range allowed by kinematics and θ_c is the maximum angle under which the outgoing electrons (positrons) are tagged. In our LEP2 analysis, we choose $\theta_c = 30$ mrad. All calculations are performed at NLO in the $\overline{\text{MS}}$ renormalization and factorization scheme using the two-loop formula for α_s . The DR and RR cross sections are calculated using the photon PDF's of Glück, Reya, and Vogt [6] transformed to the $\overline{\text{MS}}$ scheme. The renormalization and factorization scales are set to $\mu = \sqrt{p_\perp^2 + m^2}$. It is clear that in the massive scheme only three flavours are active in the initial state and in the evaluation of α_s , whereas in the massless scheme also the charm distribution in the photon contributes to charm quark production, and α_s is calculated using four active flavours. In the massive calculation and in the PFF's, we set $m = 1.5$ GeV.

In Figs. 1a–d, we show the DD, DR, and RR contributions to the cross section $d^2\sigma/dy dp_\perp^2$ as a function of p_\perp for rapidity $y = 0$ and their sum, respectively, both in the massless and massive schemes. However, one should bear in mind that, beyond LO, the separation into the DD, DR, and RR channels depends on the factorization scheme and scale and has no direct physical meaning. [As we have discussed above the DD channel in the massive scheme carries unambiguous physical meaning.] Nevertheless, we consider these channels separately in order to assess their relative importance. As may be seen from these figures, the cross section in the considered p_\perp range is dominated by the DD contribution. For the DD and DR components, the massless and massive calculations are very similar, whereas in the RR case the massive prediction is at least one order of magnitude smaller than the massless one. Comparing the two schemes, we see that the difference is somewhat larger for the DD contribution than for the DR one. In both cases, the massive cross

section exceeds the massless one, which is still the case for the total sum. The discrepancy increases for increasing p_{\perp} . The situation for the DR and RR contributions is comparable to what we have observed for photoproduction of charm quarks at HERA [17,18]. However, due to the DD channel, which does not exist in photoproduction at HERA, the total $\gamma\gamma$ results in the massless and massive schemes exhibit a pattern somewhat different from [17,18]. In total, we observe that the massless prediction for the total sum is smaller than the massive one, in particular for large p_{\perp} . We attribute this to the presence of higher-order leading-logarithmic terms in the PFF's incorporated in the massless approach, which soften the p_{\perp} distribution of the heavy quark.

We now repeat the analysis of Fig. 1 for the y spectrum at $p_{\perp} = 10$ GeV and display the DD, DR, and RR contributions as well as the total sum in Fig. 2a–d, respectively. Comparing the results in the massive and the massless approaches, we observe a pattern similar to the p_{\perp} distribution. For given p_{\perp} , the kinematically allowed y range in the massless theory is larger than that in the massive theory. This does not show up in Figs. 2a, b, and d due to the influence of the PFF's. Moreover, at the edges of phase space, where only soft-gluon emission is allowed, the PFF's are not reliable due to the missing resummation of Sudakov terms. In the region of large cross section, the shapes for the two approaches are very similar.

Next, we consider the predictions for the NLC with TESLA architecture. It is well known [25] that, at the NLC, photons are produced not only by bremsstrahlung but also via synchrotron radiation emitted by one of the colliding bunches in the field of the opposing one. This phenomenon is called beamstrahlung. The details of the beamstrahlung spectrum crucially depend on the design and operation of the NLC. For certain NLC concepts, beamstrahlung can jeopardize the overall physics potential due to severe smearing and lowering of the available centre-of-mass energy. In our study, we select the TESLA design, where the unwanted effects of beamstrahlung are reduced to an almost unnoticeable level. We coherently superimpose the WWA and beamstrahlung spectra. We compute the WWA spectrum from Eq. (2) with $\theta_c = 175$ mrad and the beamstrahlung spectrum from the expression given in [25], with parameters $\Upsilon_{\text{eff}} = 0.039$ and $\sigma_z = 0.5$ mm [26]. The p_{\perp} distributions for $y = 0$ and $\sqrt{s} = 500$ GeV are shown in Figs. 3a–d, again for the DD, DR, and RR components, and their sum, respectively. Apart from an overall enhancement due to the increased WWA logarithm, the p_{\perp} spectra exhibit features very similar to the LEP2 case, including the relation between the massless and massive approaches. The corresponding y spectra are shown in Figs. 4a–d. Due to the admixture of beamstrahlung, their shape differs from that of the pure WWA case in Figs. 2a–d. This difference is most pronounced in the DD contribution, shown in Fig. 4a, which also governs the shape of the total sum.

To achieve the highest possible photon energies with large enough luminosity, it has been proposed to convert the NLC into a $\gamma\gamma$ collider via backscattering of the e^+ and e^- beams on high-energetic laser light [3]. The corresponding photon spectrum is given by [3]

$$f_{\gamma}(x) = \frac{1}{G(\kappa)} \left(1 - x + \frac{1}{1-x} - \frac{4x}{\kappa(1-x)} + \frac{4x^2}{\kappa^2(1-x)^2} \right),$$

with

$$G(\kappa) = \left(1 - \frac{4}{\kappa} - \frac{8}{\kappa^2} \right) \ln(1 + \kappa) + \frac{1}{2} + \frac{8}{\kappa} - \frac{1}{2(1 + \kappa)^2}. \quad (3)$$

Notice that this spectrum extends only up to $x_{\text{max}} = \kappa/(1 + \kappa)$. In order to avoid the production of e^+e^- pairs in the collisions of the primary laser photons and the high-energetic back-scattered

photons, one needs to arrange the experimental set-up so that $\kappa \lesssim 4.83$. In our analysis, we choose $\kappa = 4.83$, so that $x_{\max} = 83\%$. In Figs. 5a–d, we show the p_{\perp} distributions for $y = 0$ due to the DD, DR, and RR channels, and the total sum, respectively. Compared to the previous cases, the relative magnitudes of the DD, DR, and RR components have changed. At small p_{\perp} , around 5 GeV say, the massive cross section is dominated by the DR component, which makes up approximately 60% of the total sum, while the DD component is completely negligible. At the same p_{\perp} values in the massless case, RR is the largest component, being 65% of the full result. The DD contribution is again negligible. The massless cross section is only slightly larger than the massive one. At large p_{\perp} , at around 20 GeV, the situation is different. In the massless case, the DD, DR, and RR components all have the same order of magnitude. In the massive case, the RR contribution is small, and the total cross section is built up by the DR and DD contributions approximately in the ratio 3:1. Looking at Fig. 5d, we see that p_{\perp} distributions in the two schemes almost coincide. However, the massless result falls off somewhat more strongly with p_{\perp} increasing. As may be expected, in both schemes, the DD contributions are insignificant in the low- p_{\perp} range but become important for high p_{\perp} . The corresponding y spectra for $p_{\perp} = 10$ GeV are plotted in Figs. 6a–d. As far as the relative importance of the individual contributions in the two schemes is concerned, we recognize the same pattern as in Figs. 5a, b, and c, which refer to $y = 0$. The line shapes are completely different from those encountered in the TESLA case. The y spectrum of the total sum peaks near the phase-space boundaries. This is caused by the different photon spectrum, which is now peaked at the upper edge. By contrast, the numerically small DD contribution is almost y independent. Although the total sums in the massless and massive calculations have different decompositions, they nevertheless agree very well with each other over the full y range.

Finally, we investigate the scale dependence of our results. To this end, we introduce a dimensionless scale parameter ξ and set all scales equal to $\xi\sqrt{m^2 + p_{\perp}^2}$. In Fig. 7, we plot, versus ξ , the massless and massive cross sections at $y = 0$ and $p_{\perp} = 20$ GeV for LEP2, TESLA, and Laser spectrum. For $0.5 < \xi < 2$, we observe minor scale variations, below 15%. As expected, the scale dependence is somewhat reduced in the massless cross section. We checked that the situation is similar for $p_{\perp} = 10$ GeV.

4. Conclusions

In this paper, we compared two approaches, the massless and massive schemes, for calculating inclusive charm quark production in three different arrangements of $\gamma\gamma$ reactions. The cross sections were computed at NLO, with PFF's included in the massless case. Comparing the massless and massive results in the DD, DR, and RR channels, we found essential differences, which are compensated to a large extent in their sums.

In all three arrangements, the cross section at large p_{\perp} was found to be somewhat larger in the massive case. This is in line with the findings of [16] for bottom hadroproduction and of [18] for photoproduction at HERA. In the latter case, too, it was observed that, in the massless approximation, the direct and resolved contributions, which in our case correspond to the DR and RR contributions, are comparable. On the other hand, the resolved contribution of the massive calculation was found to be suppressed [17,18], which also agrees with our $\gamma\gamma$ results.

Concerning the small p_{\perp} region, we notice that the total massless result usually overshoots the

massive one. This is due to the missing mass terms in the massless approach, which render it less reliable in this region. This effect is enhanced with respect to what was observed in [18], for the following two reasons: In this work, we use massless kinematics, whereas, in [18], massive kinematics was employed. Moreover, in [18], the photon PDF set ACFGP–ho (mc) [7] was used. In contrast to GRV used here, in this set, the massive Bethe-Heitler formula is built in for the starting condition of the charm PDF of the photon. This had the effect that, especially in the low- p_{\perp} region, the cross section was reduced.

In conclusion, we have found that, in the region of common validity, the massive and the massless approaches yield comparable results and display similar scale dependences. In the large p_{\perp} region, the massless approach predicts a lower cross section, due to the resummation of $\alpha_s \ln(p_{\perp}^2/m^2)$ terms, and leads to a reduced sensitivity to the choice of the renormalization and factorization scales.

ACKNOWLEDGMENTS

We thank P. Nason for providing us with a computer program for the evolution of the PFF's. One of us (G.K.) thanks the Theory Group of the Werner-Heisenberg-Institut for the hospitality extended to him during a visit when this paper was finalized.

References

- [1] W. Bartel et al. (JADE Collaboration), Phys. Lett. B184 (1987) 288; W. Braunschweig et al. (TASSO Collaboration), Z. Phys. C47 (1990) 499; M. Alston-Garnjost et al. (TPC/ 2γ Collaboration), Phys. Lett. B252 (1990) 499; R. Enomoto et al. (TOPAZ Collaboration), Phys. Rev. D50 (1994) 1879, Phys. Lett. B328 (1994) 535; S. Uehara et al. (VENUS Collaboration), Z. Phys. C63 (1994) 213; T. Aso et al. (AMY Collaboration), Preprint KEK–95–19; D. Buskulic et al. (ALEPH Collaboration), Phys. Lett. B255 (1995) 595; M. Iwasaki for the TOPAZ Collaboration, to appear in Proc. of *Photon '95*, Sheffield, England, 1995; T. Nozaki for the AMY Collaboration, *ibid.*; F. Foster for the ALEPH Collaboration, *ibid.*
- [2] M. Drees, M. Krämer, J. Zunft, and P.M. Zerwas, Phys. Lett. B306 (1993) 371.
- [3] I.F. Ginzburg, G.L. Kotkin, S.L. Panfil, V.G. Serbo, and V.I. Telnov, Nucl. Instr. and Meth. 219 (1984) 5.
- [4] T.F. Walsh and P.M. Zerwas, Phys. Lett. B44 (1973) 195; E. Witten, Nucl. Phys. B120 (1977) 189.
- [5] M. Drees and K. Grassie, Z. Phys. C28 (1985) 451; L.E. Gordon and J.K. Storrow, Z. Phys. C56 (1992) 307; G.A. Schuler and T. Sjöstrand, Z. Phys. C68 (1995) 607.
- [6] M. Glück, E. Reya, and A. Vogt, Phys. Rev. D46 (1992) 1973.
- [7] P. Aurenche, P. Chiappetta, M. Fontannaz, J.Ph. Guillet, and E. Pilon, Z. Phys. C56 (1992) 589.
- [8] J.C. Collins, D.E. Soper, and G. Sterman, Nucl. Phys. B263 (1986) 37.
- [9] M. Drees and R. Godbole, Nucl. Phys. B339 (1990) 355 and references therein.

- [10] P. Nason, S. Dawson, and R.K. Ellis, Nucl. Phys. B303 (1988) 607.
- [11] P. Nason, S. Dawson, and R.K. Ellis, Nucl. Phys. B327 (1988) 49.
- [12] R.K. Ellis and P. Nason, Nucl. Phys. B312 (1989) 551; W. Beenakker, H. Kuijf, W.L. van Neerven, and J. Smith, Phys. Rev. D40 (1989) 54; J. Smith and W.L. van Neerven, Nucl. Phys. B374 (1992) 36.
- [13] M. Krämer, to appear in Proc. of *Photon '95*, Sheffield, England, 1995.
- [14] M.A.G. Aivazis, F.I. Olness, and W.K. Tung, Phys. Rev. D50 (1994) 3085; M.A.G. Aivazis, J.C. Collins, F.I. Olness, and W.K. Tung, Phys. Rev. D50 (1994) 3102; F.I. Olness and S.T. Riemersma, Phys. Rev. D51 (1995) 4746; G. Kramer, B. Lampe, and H. Spiesberger, report DESY 95-201 (1995).
- [15] B. Mele and P. Nason, Nucl. Phys. B361 (1991) 626.
- [16] M. Cacciari and M. Greco, Nucl. Phys. B421 (1994) 530.
- [17] B.A. Kniehl, M. Krämer, G. Kramer, and M. Spira, Phys. Lett. B356 (1995) 539.
- [18] M. Cacciari and M. Greco, Preprint DESY 95-103, to appear in Z. Phys. C.
- [19] B.A. Kniehl and G. Kramer, Z. Phys. C62 (1994) 53.
- [20] P. Aurenche, R. Baier, A. Douiri, M. Fontannaz, and D. Schiff, Nucl. Phys. B286 (1987) 553.
- [21] F. Aversa, P. Chiappetta, M. Greco, and J.Ph. Guillet, Nucl. Phys. B327 (1989) 105.
- [22] P. Aurenche, A. Douiri, R. Baier, M. Fontannaz, and D. Schiff, Z. Phys. C29 (1985) 423.
- [23] L.E. Gordon, Phys. Rev. D50 (1994) 6753.
- [24] S. Frixione, M.L. Mangano, P. Nason, and G. Ridolfi, Phys. Lett. B319 (1993) 339.
- [25] T. Barklow, P. Chen, and W. Kozanecki, in *Proceedings of the Workshop on e^+e^- Collisions at 500 GeV: The Physics Potential*, edited by P.M. Zerwas, DESY Orange Report No. 92-123B (1992) p. 845; P. Chen, T. Barklow, and M. Peskin, Phys. Rev. D49 (1994) 3209.
- [26] D. Schulte, private communication.

FIGURE CAPTIONS

Fig. 1a–d Inclusive cross section $d^2\sigma/dy dp_{\perp}^2$ for $e^+e^- \rightarrow e^+e^-c/\bar{c} + X$ as a function of p_{\perp} for $\sqrt{s} = 175$ GeV (LEP2) and $y = 0$ in the massless (solid lines) and massive (dashed lines) schemes: (a) DD, (b) DR, (c) RR, and (d) total sum.

Fig. 2a–d Inclusive cross section $d^2\sigma/dy dp_{\perp}^2$ for $e^+e^- \rightarrow e^+e^-c/\bar{c} + X$ as a function of y for $\sqrt{s} = 175$ GeV (LEP2) and $p_{\perp} = 10$ GeV in the massless (solid lines) and massive (dashed lines) schemes: (a) DD, (b) DR, (c) RR, and (d) total sum.

Fig. 3a–d Same as Fig. 1a–d for $\sqrt{s} = 500$ GeV (NLC with WWA plus beamstrahlung).

Fig. 4a–d Same as Fig. 2a–d for $\sqrt{s} = 500$ GeV (NLC with WWA plus beamstrahlung).

Fig. 5a–d Same as Fig. 1a–d for $\sqrt{s} = 500$ GeV (NLC with laser spectrum).

Fig. 6a–d Same as Fig. 2a–d for $\sqrt{s} = 500$ GeV (NLC with laser spectrum).

Fig. 7a–c Scale dependence of $d^2\sigma/dy dp_{\perp}^2$ for $e^+e^- \rightarrow e^+e^-c/\bar{c} + X$ at $y = 0$ and $p_{\perp} = 20$ GeV in the massless (solid lines) and massive (dashed lines) schemes: (a) $\sqrt{s} = 175$ GeV (LEP2), (b) $\sqrt{s} = 500$ GeV (NLC with WWA plus beamstrahlung), and (c) $\sqrt{s} = 500$ GeV (NLC with laser spectrum). The renormalization and factorization scales are identified and set equal to $\xi\sqrt{p_{\perp}^2 + m^2}$.

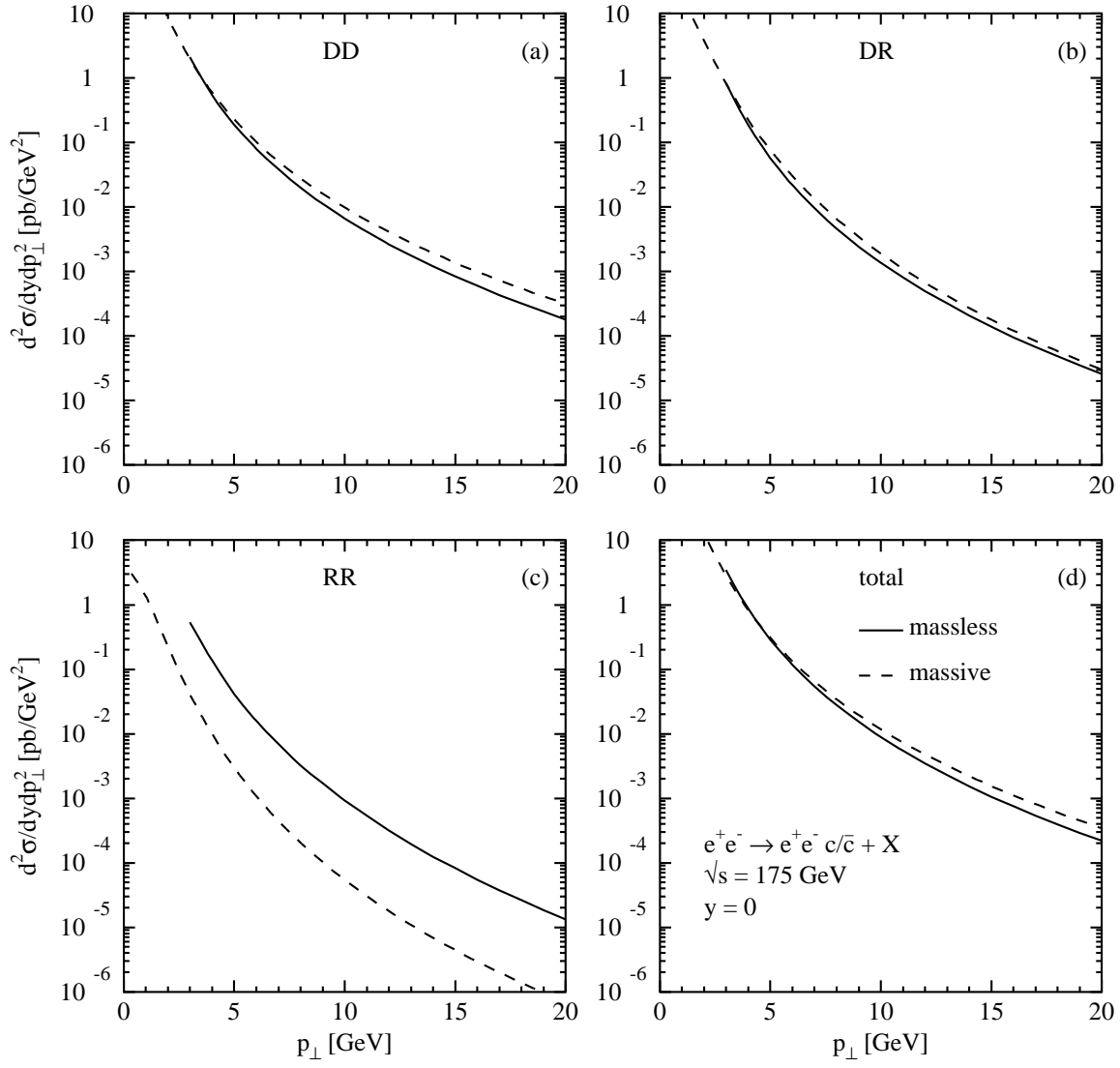


Fig. 1

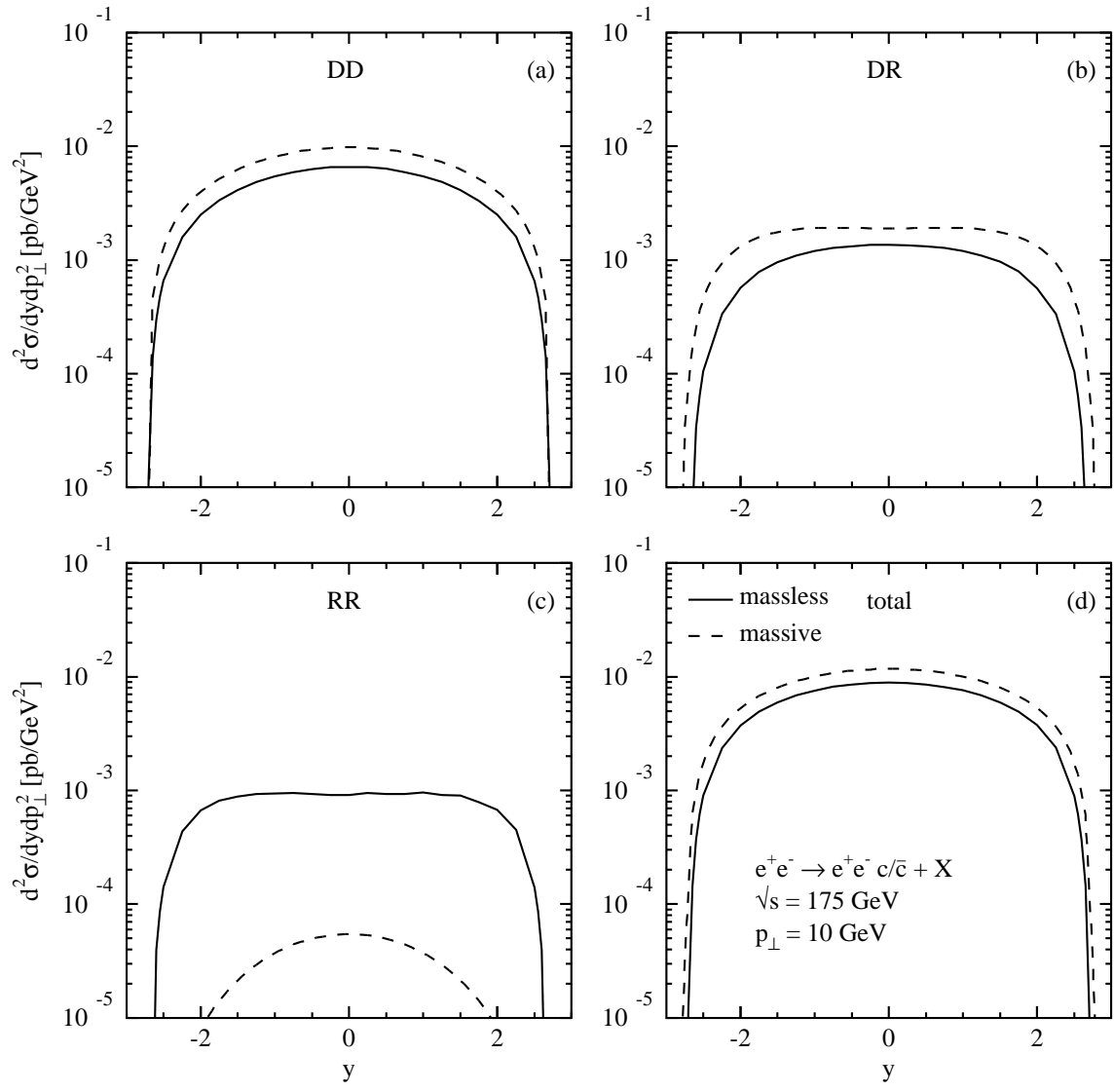


Fig. 2

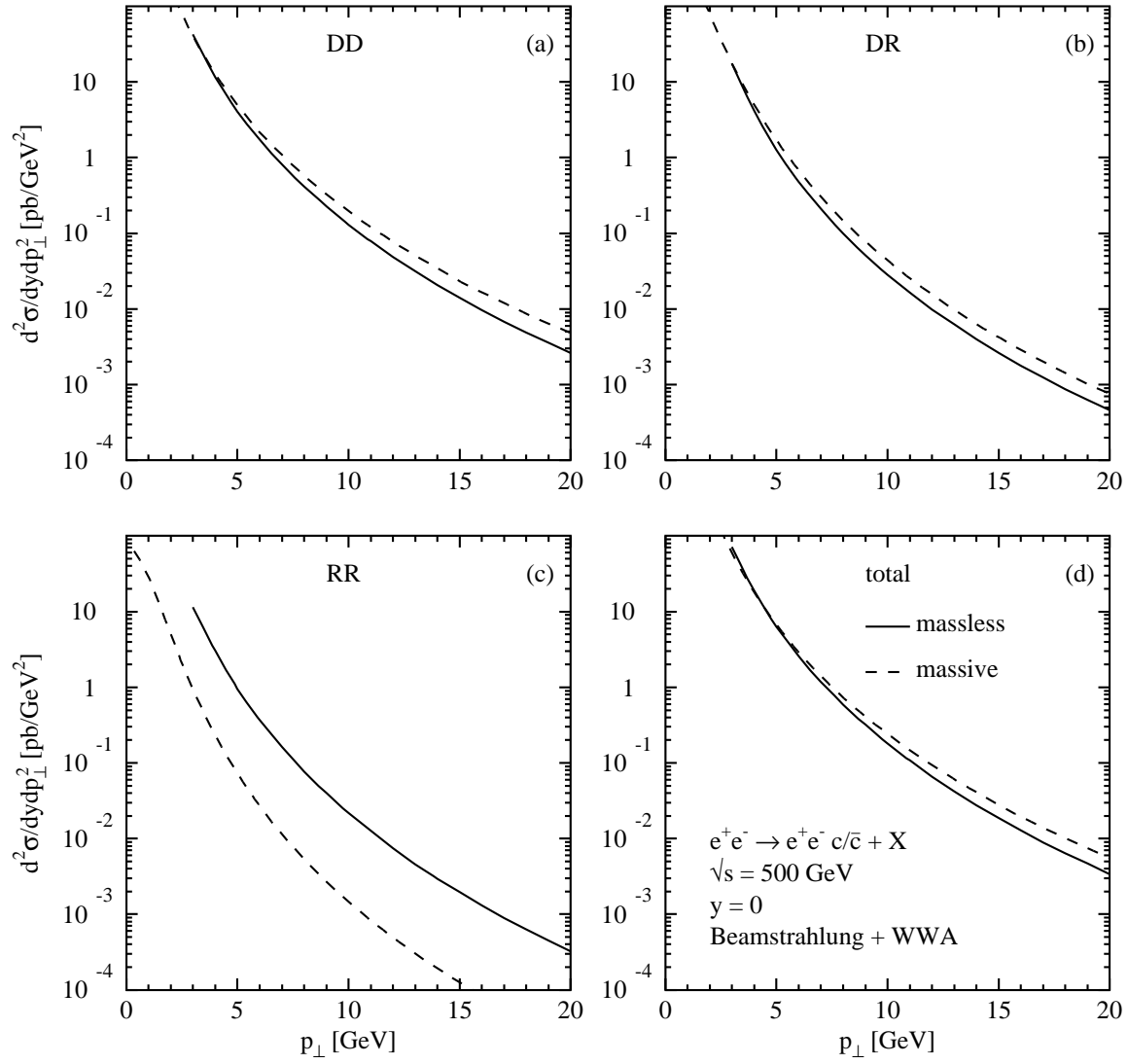


Fig. 3

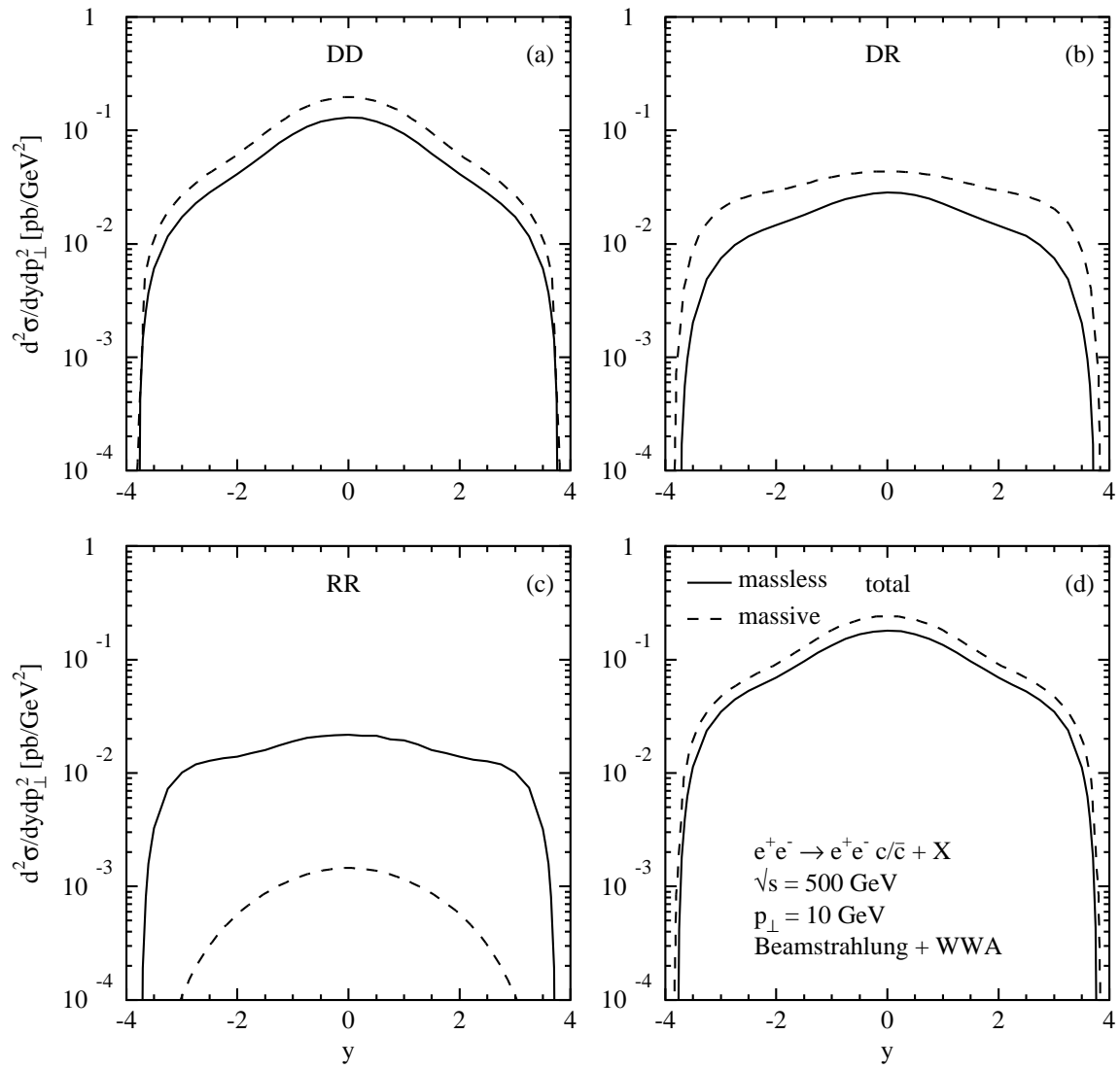


Fig. 4

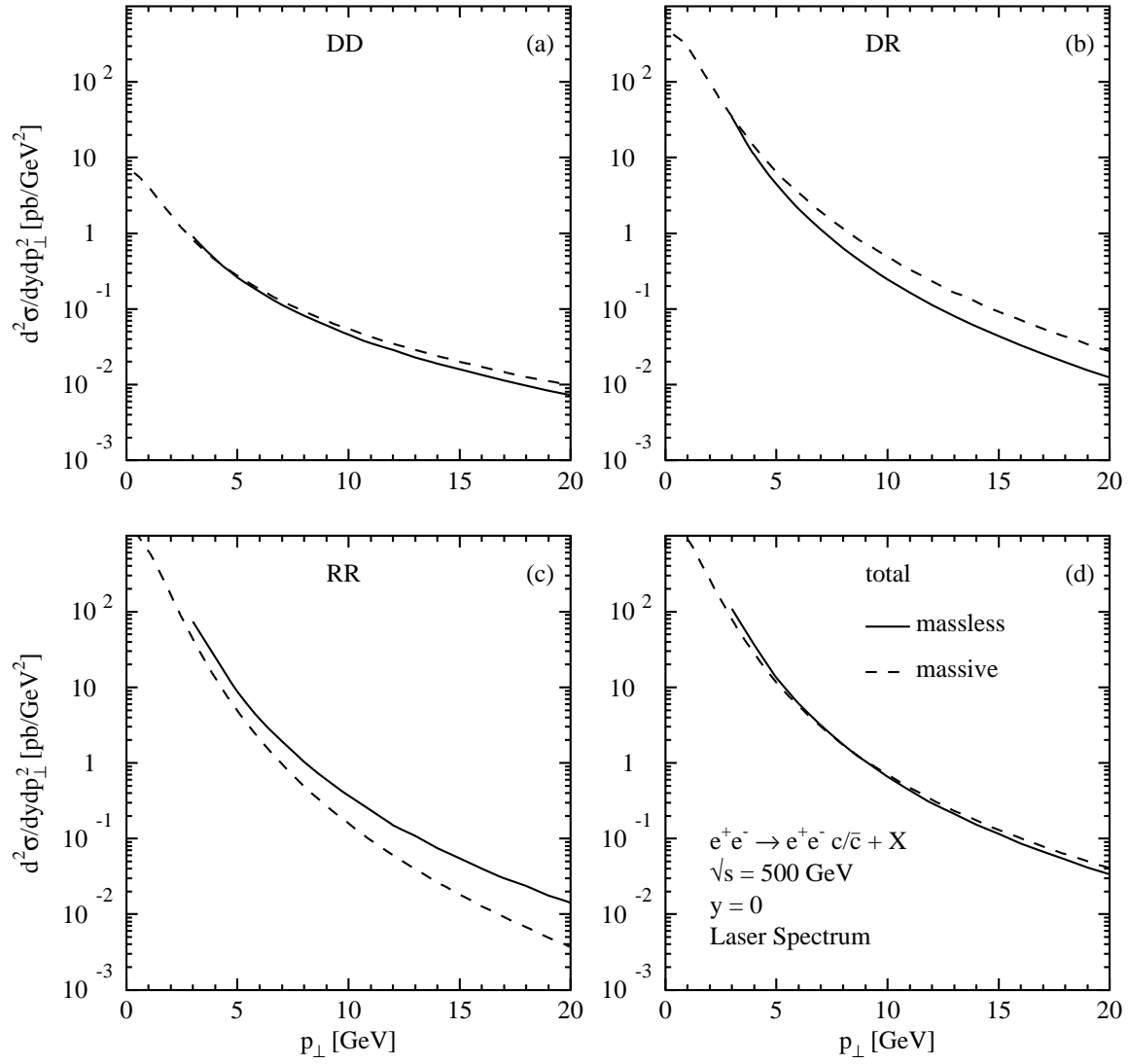


Fig. 5

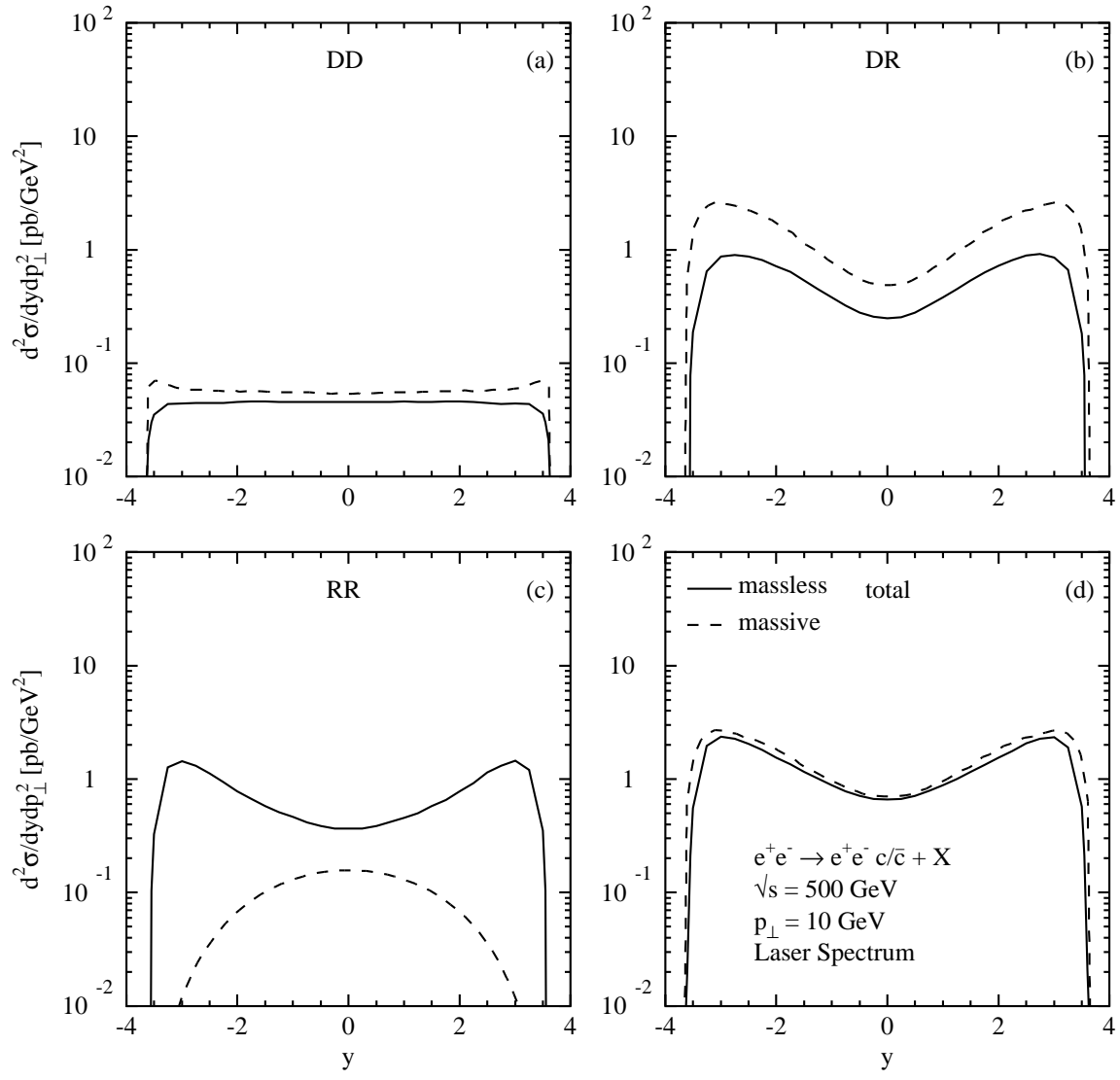


Fig. 6

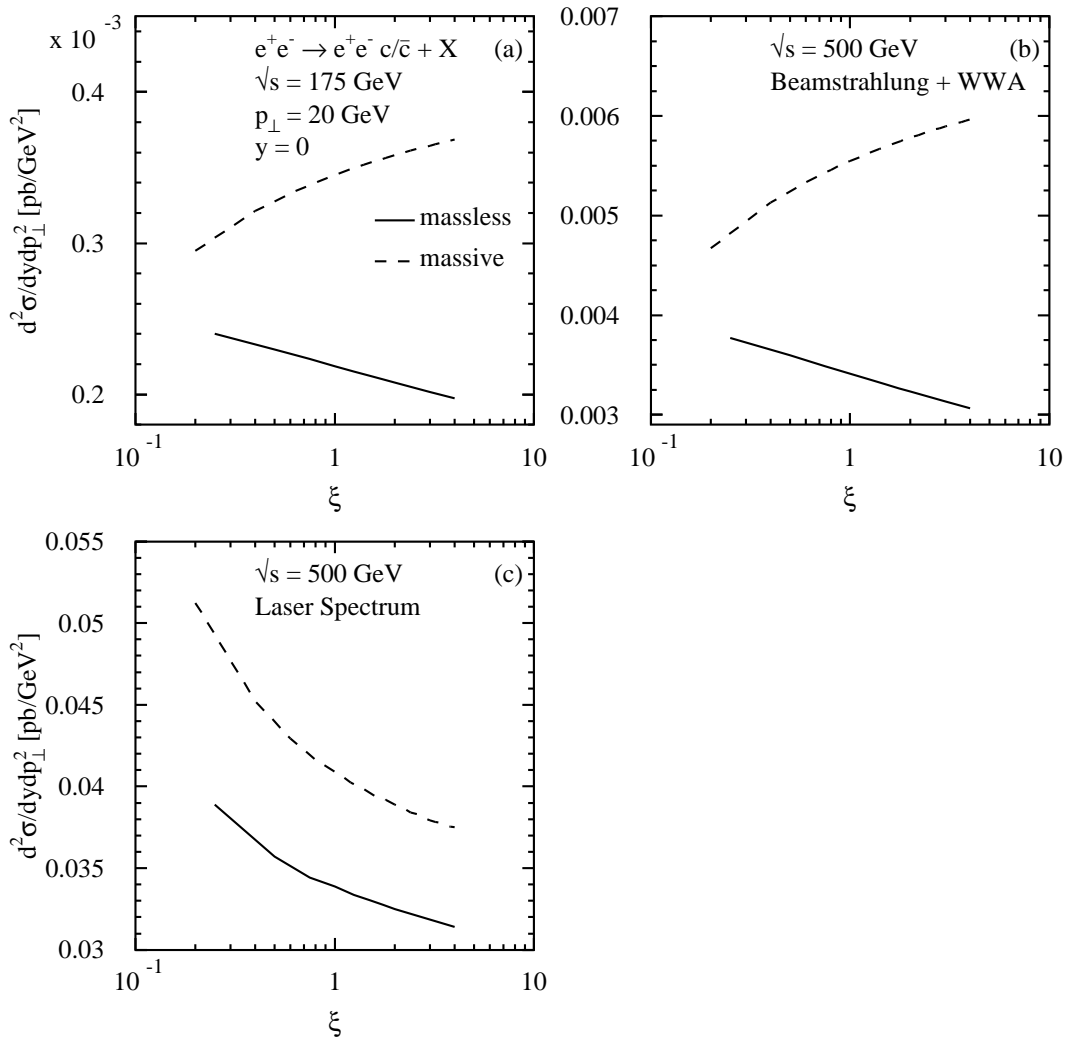


Fig. 7